ELSEVIER

Ceramics International 30 (2004) 715–720

CERAMICS INTERNATIONAL

www.elsevier.com/locate/ceramint

Chemical synthesis and characterization of nanocrystalline $ABi_2Ta_2O_9$ (A = Sr, Ba and Ca) powders

Asit Baran Panda, Abhijit Tarafdar, Amita Pathak, Panchanan Pramanik*

Department of Chemistry, Indian Institute of Technology, Kharagpur 721302, West-Bengal, India

Received 26 February 2003; received in revised form 26 March 2003; accepted 20 August 2003

Available online 5 March 2004

Abstract

Nanocrystalline $ABi_2Ta_2O_9$ (A = Sr^{2+}/Ba^{2+}/Ca^{2+}ion) powders have been prepared through decomposition of mixed metal complexes based aqueous precursor solution. Calcination of the resultant carbonaceous residue at 700–750 °C for 2 h yield the single-phase $ABi_2Ta_2O_9$ powders with average crystallite size ~12–17 nm. The relative densities of the powders, after compaction and sintering at 950 °C for 4 h, have been found to be 96.1, 96.7 and 97.6% of their theoretical values for the Ca, Ba and Sr compositions, respectively. The dielectric constant values (at 100 kHz) for the sintered pellets of Ba and Sr compositions have been found to be 1165 and 1387 at their respective Curie temperatures (T_c) of 40 and 279 °C. The T_c for the $CaBi_2Ta_2O_9$ composition has been found to be greater than 500 °C.

Keywords: A. Powders: chemical preparation; C. Dielectric properties; D. Tantalates; Nanocrystalline powders; Bismuth

1. Introduction

Ferroelectrics, which can retain their polarization state after the removal of applied field, have been intensively investigated for application in nonvolatile ferroelectric random access memory (FeRAM) [1]. To date, lead zirconate titanates (PZT) are the most widely used ferroelectric materials for such applications. However, extensive exploitation of PZT gets restricted due to their serious degradation switching characteristics, i.e. fatigue [2]. Since polarization must be reversed to read or write data in memory cells, hence 'fatigue' poses as a crucial deterrent in memory device applications.

Of late, the bismuth-based layered perovskite-type compounds have gained attention as leading entrants for FeRAM applications because of their excellent fatigue endurance even after 10^{12} cycles of operation [3,4]. These Aurivillius compounds were first discovered by Aurivillious in 1949 [5] and their ferroelectric properties and basic structures were studied by Subbarao [6] and Smolenskii et al. [7] in the early 60s. Among these Bi-based layered compounds, $SrBi_2Ta_2O_9$ (SBT) is the most extensively studied ferroelectric compound for the use in memory device as they possess excellent fatigue free properties. The crystalline structure of SBT belongs to the layered type perovskite ferroelectrics [5] where the crystal consists of stacks of alternating layers of Bi_2O_2 and pseudo-perovskite $SrTa_2O_7$ units with double TaO_6 octahedral (i.e. $SrTa_2O_7$) layers along the *c*-axis. Neutron and electron diffraction studies reveal that the SBT structure has orthorhombic distribution with space group $A2_1am$ [8]. The presence of Bi_2O_2 layers has been thought to serve as shock absorbers for enduring the polarization fatigue [9].

However, widespread application and commercialization of the bismuth layered perovskite ferroelectrics have so far been limited by their relatively low remnant polarization [10,11] and high processing temperatures that sets off volatilization of bismuth from the system. Efforts to enhance the properties of these layered ferroelectrics by the addition or substitution of alternative metal ion or by improving its particle morphology have been reported [8,12] recently.

Our previous studies [13] on dielectric properties of stoichiometric and off stoichiometric SBT compositions ($Sr_{1-x}Bi_{2+y}Ta_2O_9$) revealed that the cation substitution (by Bi^{3+} ions) at the Sr-site significantly influenced the remnant polarization of the material. Cation substitution at Sr-site led to larger ferroelectric polarization and higher ferroelectric Curie temperature in the sintered materials and thus significantly influenced their ferroelectric properties compared

* Corresponding author. Tel.: +91-3222-83322; fax: +91-3222-55303.
E-mail address: asitp@chem.iitkgp.ernet.in (P. Pramanik).

0272-8842/$30.00 © 2004 Published by Elsevier Ltd and Techna Group S.r.l.
doi:10.1016/j.ceramint.2003.08.010

to that of the reported bulk materials [14]. In the present investigation, Sr^{3+} ions in the SBT composition have been independently replaced by Ca^{2+} and Ba^{2+} ions and their dielectric properties have been measured after sintering.

The ferroelectric properties of ceramic materials, such as SBT, strongly depend on their homogeneity and morphology hence, the wet or, solution-based chemical routes are considered appropriate for their synthesis. The solution-based chemical routes not only reduces the processing temperatures for material synthesis but they can also efficiently control the morphology, chemical homogeneity and stoichiometry of the material through molecular level mixing of the starting compounds in a solution [15,16]. In most of the reported wet or chemical processes, metal alkoxides and metal halides have been used as the starting materials, which are expensive and moisture sensitive.

In the present study, we report a novel chemical route for the preparation of single-phase, nanocrystalline $ABi_2Ta_2O_9$ (where A = Ca^{2+}, Ba^{2+}, Sr^{2+}) powders starting from aqueous precursor solutions of complexes of the respective metal ions and triethanolamine (TEA). In this method tantalum–tartarate complex has been used as the source of tantalum, which overcomes the problem of moisture sensitivity. The route involved the decomposition of aqueous precursor solution to obtain a carbonaceous precursor mass, which resulted in nanosized powders after calcination. The final powders have been investigated through X-ray powder diffraction (XRD), transmission electron microscopy (TEM) and dielectric measurements.

2. Experimental procedure

The raw materials, used for the preparation of the $ABi_2Ta_2O_9$ (where A = Ca^{2+}, Ba^{2+}, Sr^{2+}) were $Sr(NO_3)_2$, $Ba(NO_3)_2$, $Bi(NO_3)_3$, EDTA, TEA and tantalum tartarate. The aqueous based precursor solution for the preparation of the $ABi_2Ta_2O_9$ was composed of TEA complex of bismuth (i.e. Bi–TEA), EDTA complex of $Ca^{2+}/Ba^{2+}/Sr^{2+}$ and tartarate complex of tantalum. A stock of aqueous solution of Bi–TEA complex was freshly prepared by mixing TEA (2 M) and aqueous solution of bismuth nitrate (1 M). Similarly, aqueous stock solutions of the EDTA complexes were separately prepared by mixing aqueous solutions of $Sr(NO_3)_2/Ba(NO_3)_2/Ca(NO_3)_2$ (1 M) and ammoniacal EDTA (1 M). The solution of the tantalum–tartarate complex was prepared in the laboratory from its hydrated oxide ($Ta_2O_5{\cdot}nH_2O$) and the details of the preparation process is discussed elsewhere [13].

Stoichiometric amounts of these metal complex solutions were taken from their respective stocks and mixed together with continuous stirring to obtain a clear solution of the $Ca^{2+}/Ba^{2+}/Sr^{2+}$–EDTA and Bi–TEA complexes. Stoichiometric amount of the prepared tantalum–tartarate complex solution was then introduced into the solution mixture, followed by the addition of optimum amounts of TEA (∼5 mol per unit mole of the total metal ions). The solution mixture of the cationic complexes was constantly stirred resulting in a red, homogeneous precursor solution.

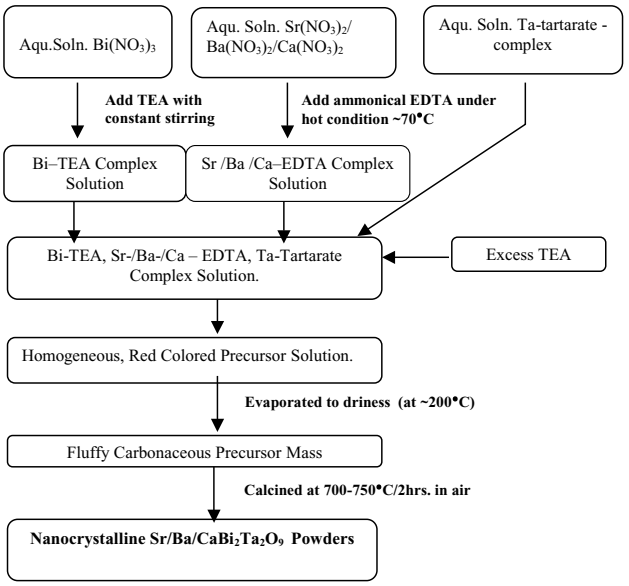

Fig. 1. Schematic representation of the precursor solution method for the synthesis of $Sr/Ba/CaBi_2Ta_2O_9$ powders.

The resultant red colored precursor solution was heated over a hot plate (at ∼200 °C) for complete evaporation. On complete dehydration of the precursor solution, TEA and the metal complexes decomposed with the evolution of dense fumes and resulted in a voluminous, fluffy, black organic mass. The fluffy precursor material was ground to powder and was calcined at 700–750 °C for 2 h to obtain the desired layered perovskite phase. The entire preparative process has been illustrated in Fig. 1.

The nanocrystalline powders of all the different three compositions (i.e. $SrBi_2Ta_2O_9$, $BaBi_2Ta_2O_9$ (BBT), and $CaBi_2Ta_2O_9$ (CBT)), which were obtained on calcination of the respective precursor powders at their phase formation temperatures, were then compacted into pellets under uniaxial pressure of 3.2×10^7 Pa and then sintered at 950 °C for 4 h. The pellet densities were measured using Archimedes' method, and for calculating the theoretical densities, all the XRD peaks for the samples were indexed and the lattice parameters were calculated using a computer package based on least-square refinement method. For carrying out the dielectric studies, both flat surfaces of the sintered pellets were polished and electroded by applying silver paste and the variations of the dielectric constant (ε) with temperature was measured at a constant frequency of 100 kHz.

3. Characterization of materials

Simultaneously recorded thermogravimetric and differential thermal analysis (TG/DTA) (model: Shimadzu DT-40, Japan) of the precursor powders were carried out

in air at a heating rate of 5 °C/min. The X-ray diffraction (model: Philips P.W. 1710, Holland) of the precursor and heat-treated powders were studied using Cu Kα radiation. The microstructure and particle-size studies in the final powders were carried out on a transmission electron microscope (TM-300, Phillips, Holland). Dielectric properties of the sintered pellets have been measured using a capacitance-measuring assembly (model AP-1620, GRC).

4. Results and discussions

4.1. Thermal studies

The DTA curves revealed similar single step, exothermic thermal affects for all the $ABi_2Ta_2O_9$ (where A = Ca^{2+}, Ba^{2+}, Sr^{2+}) precursors, with the exothermic peak appearing around 400–450 °C. The exotherm could be assigned to the oxidation of the carbonaceous residuals that were retained in the precursor material on decomposition of the metal complexes and TEA. The entire thermal affect was accompanied by the evolution of various gases, such as CO, CO_2, NH_3, water vapor, etc. which was manifested by a single step weight loss in the TG curve. Above 750 °C, there was no significant thermal effect observed in DTA curves and the corresponding TG curves showed no weight loss, implying the formation of the oxides phase at this temperature. The DTA/TG curves for $CaBi_2Ta_2O_9$ precursors are depicted in Fig. 2 as a typical representative.

4.2. X-ray diffraction studies

To study the influence of heat-treatment temperatures on the formation of the layer-perovskite phase, the virgin precursors of all the three compounds (SBT, BBT, CBT) were heat-treated at various temperatures ranging between 400 and 900 °C for 2 h. Room temperature XRD studies revealed that the virgin precursors were amorphous and continued to remain so up to the heat-treatment temperatures of 400 °C. Crystallization of the intermediate fluorite phase [17] initiated at 500 °C for 2 h. Heat-treatment of the precursors at

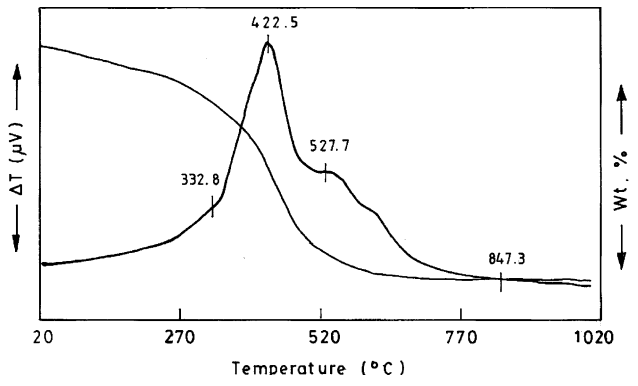

Fig. 2. Thermal studies of the $CaBi_2Ta_2O_9$ precursors powders.

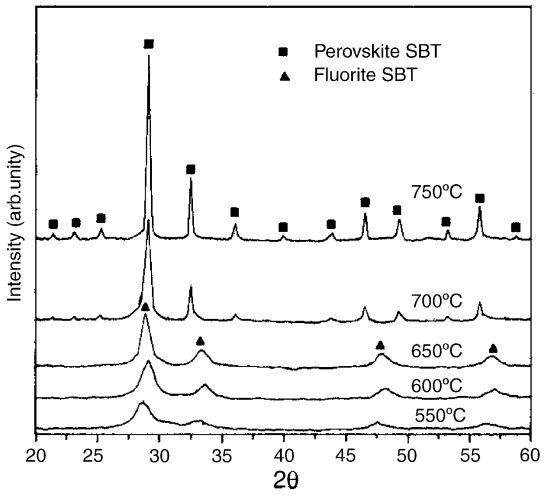

Fig. 3. Room-temperature X-ray powder diffractograms (using Cu Kα radiation) of the SBT precursors on heat-treatment for 2 h at different temperatures.

600–650 °C for 2 h was marked by the appearance of diffraction lines characteristic of the perovskite phase in addition to the fluorite phase. The mixed phase was eventually transformed to the respective perovskite phase on heat-treatment of the precursors at 700–750 °C. Further increase in the heat-treatment temperatures was manifested by sharpening of diffraction lines, reflecting growth in crystallinity in the samples. The X-ray diffractograms of the virgin $SrBi_2Ta_2O_9$ precursor and their respective calcined powders are depicted in Fig. 3. Crystallization of the desired perovskite phase from their respective virgin samples via the intermediate fluorite phase (no other oxide phase of constituent metal) implied that the intermediate fluorite phase is the nucleating phase for the formation of the final perovskites. Accomplishment of the pure perovskite phase at relatively low external heat-treatment temperatures indicated the presence of small atomic clusters of appropriate chemical homogeneity in the amorphous precursors, which facilitated the crystallization process through the nucleating fluorite phase. The crystallite sizes of the heat-treated powders were calculated from the X-ray broadening of the '*d*' line, using the Scherrers' equation [18] and were found to be range between 12 and 17 nm. The details of the phase formation temperature and crystallite sizes are summarized in the Table 1.

4.3. Microstructure studies

The bright field transmission electron micrograph for the representative $SrBi_2Ta_2O_9$ composition obtained after heat-treatment of the precursor powders at its crystallization temperatures (i.e. at 700 °C for 2 h) is illustrated in Fig. 4. The TEM micrographs represented the basic powder morphology in the samples, where the smallest visible isolated spot can be identified with particle/crystallite agglomerates. From the TEM study it was observed that the particles were almost spherical with average particle di-

Table 1
Comparison of the general characteristics of the prepared $ABi_2Ta_2O_9$ powders

Composition	Phase formation temperature (°C)	Average crystallite size[a] (nm)	Average particle size[b] (nm)	Relative density[c]	T_c (°C)	ε_{max}[d]
$SrBi_2Ta_2O_9$	700	12	15	97.6	279	1387
$BaBi_2Ta_2O_9$	750	18	21	96.7	40	1165
$CaBi_2Ta_2O_9$	750	17	40	96.1	>500	–

[a] The average crystallite sizes calculated using the Scherrers' formula applied to the various d_{hkl} lines of the precursor powders that were calcined at their respective phase formation temperatures.
[b] Average diameters of the smallest visible isolated particle/crystallite agglomerate as observed from TEM studies for the precursor calcined at their respective phase formation temperatures.
[c] Relative density evaluated of the pellets after sintering at 950 °C for 4 h.
[d] Value of the dielectric constant measured at their respective Curie temperature (T_c) at 100 kHz.

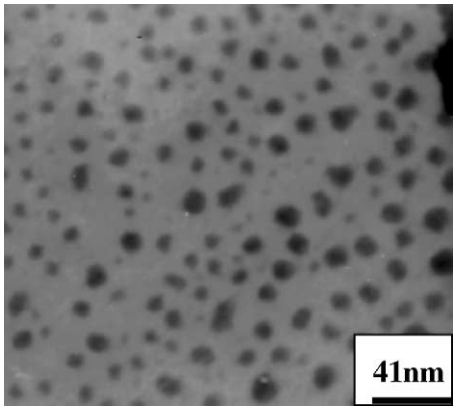

Fig. 4. Bright field transmission electron micrograph of the $SrBi_2Ta_2O_9$ samples after calcination of the precursor powders at 700 °C for 2 h.

ameters lying between 15 and 40 nm. The corresponding selected area electron diffraction pattern of the same sample (i.e. $SrBi_2Ta_2O_9$) showed distinct rings, characteristic of an assembly of nanocrystallites (Fig. 5). Average diameters of the smallest visible isolated particle/crystallite agglomerate, as observed from TEM studies, for the various precursor powders after heat-treated at their respective crystallization temperatures are given in Table 1. The values of the crystallite size and the average TEM particle size were observed to be the lowest for the $SrBa_2Ta_2O_9$ composition.

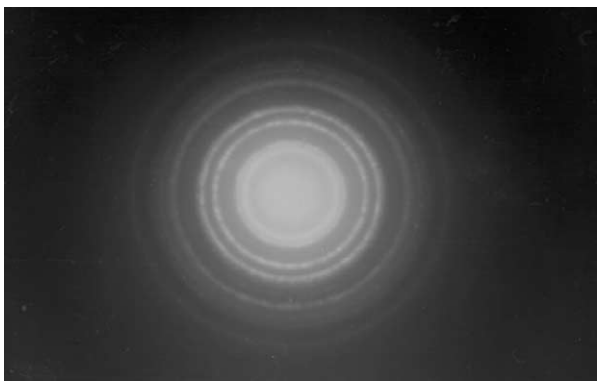

Fig. 5. The corresponding selected area electron diffraction pattern of the $SrBi_2Ta_2O_9$ powders after calcination of the precursor powders at 700 °C for 2 h.

4.4. Dielectric property studies

Studies on the variations of the dielectric constant (ε) with temperature, for each of the sintered $ABi_2Ta_2O_9$ pellets were performed and the results are depicted in Fig. 6. $SrBi_2Ta_2O_9$ exhibited dielectric behavior distinctive of normal ferroelectric materials where the ε values gradually increased with temperature and attained a maximal value (ε_{max}) at the Curie temperature (T_c) of 279 °C. The ε values above Curie temperature obeyed the Curie–Weiss law. The $CaBi_2Ta_2O_9$ composition also showed dielectric behavior typical of normal ferroelectrics, where the ε values gradually increased up to the accomplished temperatures of 500 °C.

The temperature versus ε plots for the $BaBi_2Ta_2O_9$ composition showed a broad peak around Curie temperature (40 °C). This kind of broad transition peak in ε is typical of relaxor-type ferroelectric materials, such as $PbMg_{1/3}Nb_{2/3}O_3$ [19]. A broad peak in the temperature dependence plot of ε may be attributed to minute differences in T_c values among the different microscopic ferroelectric domains, which manifests in a gradual ferroelectric transition in these types of materials.

Difference in the ferroelectric behavior of BBT to that of SBT/CBT could be attributed to their structural dissimilarities. BBT possesses a distorted pseudo-tetragonal structure with space group 14/*mmm* while SBT and CBT both,

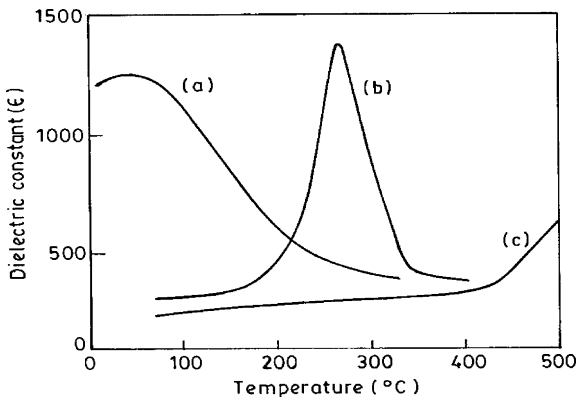

Fig. 6. Variation of dielectric constant (ε) with temperature for (a) $BaBi_2Ta_2O_9$, (b) $SrBi_2Ta_2O_9$ and (c) $CaBi_2Ta_2O_9$ systems.

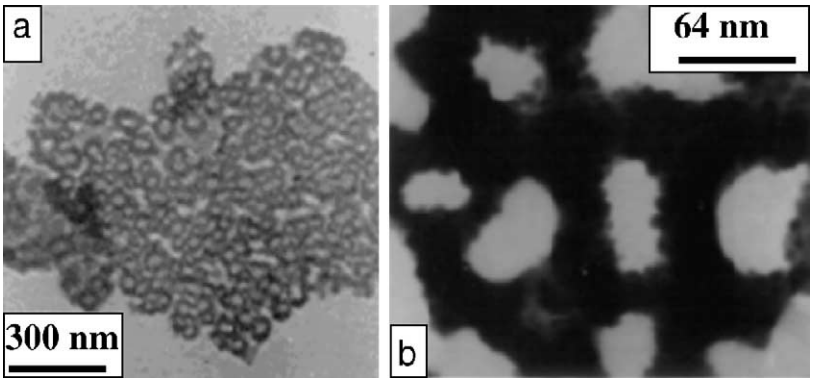

Fig. 7. (a and b) The bright field transmission electron micrograph of the dried carbonaceous precursor material for the $SrBi_2Ta_2O_9$ system taken at two different magnifications.

have a distorted orthorhombic structure with space group $A2_1am$. Such structural dissimilarity probably arises due to larger size of the Ba^{2+} ions. It is evident from Fig. 6 that as the size of the cations in the A-site decreases from Ba^{2+} to Ca^{2+}, the lattice distortion within the structure become more pronounced, which culminates in a shift in the Curie temperatures to higher values; and larger values of spontaneous ferroelectric polarization and the dielectric constant at the respective T_c.

The discussed chemical process is based on the homogeneous and atomistical distribution of the metal ions in a precursor solution, which was constituted of soluble tantalum–tartarate complex (as the tantalum source), EDTA complexes of $Sr^{2+}/Ca^{2+}/Ba^{2+}$ ions, TEA complex of bismuth and TEA. The amount of TEA in the precursor solution was always kept in excess to the total cations present in the reaction mixture (i.e. ~5 mol of TEA per unit mole of the total metal ions). TEA helped the metal ions to remain in solution and provided sufficient flexibility to the system to exist homogeneously throughout the evaporation process with out under going any precipitation and segregation.

Complete evaporation of the precursor solution resulted in a weightless, fluffy black decomposed mass, which in essence is a carbonaceous material. The BET surface area (carried out by adsorption of nitrogen gas at liquid nitrogen temperatures using micromeritics high-speed surface area analyzer) of the generated fluffy carbonaceous precursor was found to range between 160 and 200 m^2/g. TEM studies of the same precursor material showed continuous network of cage-like carbon structures with numerous voids (i.e. pores) homogeneously distributed along the units (Fig. 7a and b). The structures were observed to be free of sharpened edges with pore diameters ranging between 10 and 65 nm. The corresponding selected area electron diffraction (SAED) pattern did not show any discrete diffraction pattern inferring the glassy nature of the precursor material. Thus, based on these studies it could be presumed that the metal ions and their clusters in the precursor material essentially remained embedded in the matrix of mesoporous carbon.

Based on the experimental findings it can be presumed that the complete evaporation of the precursor solution and the consequent decomposition of the metal complexes generated, in situ, a matrix of polar mesoporous carbon enriched with oxygen atoms. The decomposition of TEA along with the metal complexes during the complete evaporation process was expected to impart a higher polarity to the mesoporous carbonaceous material due to induction of nitrogen into the matrix. These highly polar, mesoporous-carbon precursor structures probably favored the accommodation of the metal ions in its matrix. Calcination of this highly polar precursor material (at ~500 °C) led to volatilization of the residual carbon through oxidation and generated sufficient heat for the formation of the nucleating fluorite phase. Calcination at external temperatures ranging between 700 and 750 °C facilitated rearrangement of the nucleating fluorite phase and their eventual transformation into nanocrystals of the respective $ABi_2Ta_2O_9$ (where A = Ca^{2+}, Ba^{2+}, Sr^{2+}) phase. It has been an empirical observation that fluffier was the precursor material, finer were the powders obtained on heat-treatment and narrower was their grain-size distribution.

5. Conclusions

The synthesis of the pure nanocrystalline $ABi_2Ta_2O_9$ (where A = Ca^{2+}, Ba^{2+}, Sr^{2+}) powders through evaporation of a mixture of tantalum tartarate and other metal ion complex solutions followed by calcination at comparatively low temperatures (700–750 °C) has been developed. The use of soluble tantalum–tartarate as tantalum source is found to be an efficient alternative for the preparation of any tantalum based mixed oxides since it is cheap, does not involve the problems of moisture sensitivity and hydrolysis. The particle-size distribution observed in the final powders was narrow, and the average sizes ranged between 20 and 36 nm, which is much smaller than that of those obtained via other solution-based/solid-state methods. The problems of bismuth evaporation could be avoided using this process,

as the phase formation and sintering temperature were quite low, i.e. 700–750 and 950 °C, respectively.

The dielectric constant measurements revealed that SBT behaved as normal ferroelectrics while BBT showed characteristics similar to relaxor ferroelectrics. Dielectric constant and the phase transition temperatures (T_c) were observed to increase with decreasing size of the cations in the A-site cation.

Acknowledgements

The authors are grateful for the financial assistance from the Council of Scientific and Industrial Research (CSIR), Government of India for carrying out the study.

References

[1] J.F. Scott, C.A. De Araujo Paz, Ferroelectric memories, Science 246 (1989) 1400–1405.
[2] G.A.C.M. Spierings, M.J.E. Ulenaers, G.L.M. Kampscho'er, H.A.M. Van hal, P.K. Larsen, Preparation and ferroelectric properties of $PbZr_{0.53}Ti_{0.47}O_3$ thin film by spin coating and metaorganic decomposition, J. Appl. Phys. 70 (1991) 2290.
[3] C.A. De Araujo Paz, J.D. Cuchiaro, M.C. Scott, L.D. Mcmillan, Fatigue-free ferroelectric capacitors with platinum electrodes, Nature Lond. 374 (13) (1995) 627–629.
[4] J.F. Scott, F.M. Ross, C.A. De Araujo Paz, M.C. Scott, M. Hoffman, Structure and device characteristics of $SrBi_2Ta_2O_9$ based nonvolatile random access memories, MRS Bull. 21 (1996) 33–39.
[5] B. Aurivillus, Mixed bismuth oxides with layer lattices, I. The structure type of $CaNb_2Bi_2O_9$, Arkiv Fur Kemi 54 (1949) 463–480.
[6] E.C. Subbarao, A family of ferroelectric bismuth compounds, J. Phys. Chem. Solids 23 (1962) 665–676.
[7] G.A. Smolenskii, V.A. Isupov, A.I. Agranovskaya, Ferroelectrics of oxygen-octahedral type with a layer structure, Fiz. Tverdogo Tela. 3 (1961) 895–901.
[8] Y. Shimakawa, Y. Kubo, Y. Nakagawa, S. Goto, T. Kamiyama, H. Asano, F. Izumi, Crystal structure and ferroelectric properties of $ABi_2Ta_2O_9$ (A = Ca, Sr and Ba), Phys. Rev. B. 61 (10) (2000) 6559–6564.
[9] C.A. de Araujo Paz, J.D. Cuchiaro, M.C. Scott, L.D. Mcmillan, Layered superlattice material applications: Background of the invention, International Patent Wo93/12542, 1993.
[10] J.F. Scort, Layered perovskite thin films and memory devices, in: R. Ramesh (Ed.), Thin Film Ferroelectric Materials and Devices, Kluwer, Norwell, MA, 1997, p. 115.
[11] J.F. Scort, High dielectric constants thin films for dynamic random access memories (DRAM), Ann. Rev. Mater. Sci. 28 (1998) 79–100.
[12] Y. Wu, C. Nguyen, S. Seraji, M.J. Forbess, S.J. Limmer, T. Chou, G. Cao, Processing and properties of strontium bismuth vanadate niobate ferroelectrics, J. Am. Ceram. Soc. 84 (12) (2001) 2882–2888.
[13] A.B. Panda, A. Pathak, M. Nandagoswomi, P. Pramanik, Preparation and characterization of nanocrystalline $Sr_{1-x}Bi_{2+y}Ta_2O_9$ powders, Mater. Sci. Eng. B97 (2003) 275–282.
[14] J.S. Kim, C. Cheon, H.S. Shim, C.H. Lee, Crystal structure and phase transitions of $Sr_{1\pm x}Bi_{2\pm y}Ta_2O_9$ ceramics, J. Eur. Ceram. Soc. 21 (2001) 1295–1298.
[15] R.N. Das, A. Pathak, P. Pramanik, Low temperature preparation of nanocrystalline lead zirconate titanate and lead lanthanum zirconate titanate powders using triethanolamine, J. Am. Ceram. Soc. 81 (12) (1998) 3357–3360.
[16] J.C. Roy, R.K. Pati, P. Pramanik, Chemical synthesis and characterization of nanocrystalline powders of pure zirconia and yttria stabilized zirconia, J. Eur. Ceram. Soc. 20 (2000) 1289–1295.
[17] D. Nelis, K.V. Werde, D. Mondelaers, G. Vanholand, M.K.V. Bael, J. Mullens, L.C.V. Poucke, Synthesis of $Sr_2Bi_2Ta_2O_9$ (SBT) by means of a soluble Ta(V) precursor, J. Eur. Ceram. Soc. 21 (2001) 2047–2049.
[18] M.P. Klug, L.E. Alexander, X-ray Diffraction Procedure for Polycrystalline and Amorphous Material, Wiley, New York, 1974, p. 634.
[19] R.N. Das, P. Pramanik, Chemical synthesis of fine powder of lead magnesium niobate using niobium tartarate complex, Mater. Lett. 46 (1) (2000) 7–14.